GEOPHYSICAL RESEARCH LETTERS, VOL. 36, L00C05, doi:10.1029/2009GL038905, 2009

Click Here for Full Article

C/NOFS observations of intermediate and transitional scale-size equatorial spread *F* irregularities

F. S. Rodrigues,[1] M. C. Kelley,[2] P. A. Roddy,[3] D. E. Hunton,[3] R. F. Pfaff,[4] O. de La Beaujardière,[3] and G. S. Bust[1]

Received 30 April 2009; revised 11 June 2009; accepted 16 June 2009; published 6 August 2009.

[1] We present initial results of the analysis of high sampling rate (512 Hz) measurements made by the Planar Langmuir Probe (PLP) instrument and the Vector Electric Field Instrument (VEFI) onboard the Communication/Navigation Outage Forecasting System (C/NOFS) satellite. This letter focuses on the analysis of irregularities with scale-sizes in the intermediate (0.1–10 km) and transitional (10–100 m) domains observed when the satellite was flying through a large equatorial spread *F* (ESF) depletion on the night of October 9–10, 2008 over South America. The results presented in this letter suggest the operation of a diffusive subrange in the density power spectra and the possibility of an inertial plasma regime being observed at relatively low altitudes as a result of the long-lasting solar minimum conditions. **Citation:** Rodrigues, F. S., M. C. Kelley, P. A. Roddy, D. E. Hunton, R. F. Pfaff, O. de La Beaujardière, and G. S. Bust (2009), C/NOFS observations of intermediate and transitional scale-size equatorial spread *F* irregularities, *Geophys. Res. Lett.*, *36*, L00C05, doi:10.1029/2009GL038905.

1. Introduction

[2] Equatorial Spread *F* (ESF) is the general name given to the manifestation of electron density irregularities whose generation is initiated by interchange instabilities in the nighttime equatorial ionosphere. ESF has been studied for several decades using various types of radio and/or optical instruments and using advanced numerical simulations. Our understanding of the ESF dynamics has substantially increased over the years, but we still seek a better understanding of the day-to-day variability in the ESF occurrence and a better understanding of the spatial distribution of the small-scale density irregularities associated with this phenomenon.

[3] On April 16, 2008 a satellite equipped with a suite of instruments for ionospheric measurements was launched as part of the Communication/Navigation Outage Forecasting System (C/NOFS) mission of the United States Air Force (USAF). The orbit of the C/NOFS satellite has an inclination of 13°, perigee of 405 km, apogee of 853 km, and a period of approximately 93 minutes. One of the main objectives of this satellite mission is to better characterize the ESF density irregularities as a function of the various ionospheric drivers [e.g., *de La Beaujardière et al.*, 2004]. The results of this mission will improve our understanding of the evolution and decay of ESF irregularities and our understanding of the propagation of radio waves through the disturbed ionosphere. The high sampling rate of C/NOFS operation modes allow the measurement and study of intermediate (1–10 km) and transitional (10–100 m) scale-size ionospheric irregularities. These high resolution measurements can help us to identify the physical processes leading to small scale-size irregularities and improve the modeling of the propagation of radio waves through ESF.

[4] This letter presents the results of an analysis of ionospheric irregularities in the intermediate and transitional horizontal scale-size domains observed by the C/NOFS satellite during a strong ESF event over South America. The letter is organized in the following order: In Section 2 we briefly describe the instrumentation, observations, and method of analysis. In Section 3 we present some of the results of our analysis. These results are discussed in Section 4, and the main conclusions are summarized in Section 5.

2. Measurements and Analysis

[5] The C/NOFS satellite [*de La Beaujardière et al.*, 2004] is equipped with the CINDI instrument package, which includes an ion velocity meter (IVM) instrument for measurements of ion composition, temperature, and drifts, and a neutral wind meter (NWM), for measuring the neutral density and velocity. The satellite also has a radio occultation receiver for ionospheric sensing and specification (CORISS), and the Naval Research Laboratory (NRL) Coherent Electromagnetic Radio Tomography (CERTO) beacon for measurements of plasma density profiles and phase and amplitude scintillation. In addition, C/NOFS is equipped with a Planar Langmuir Probe (PLP) instrument package for measurements of ion density and electron temperature, and with a vector electric field instrument (VEFI) package, which is formed by 6 electric field booms, a 3-axis magnetometer, and a lightning detector. For this study, we used the high sampling rate (512 Hz) ion density measurements made by the Planar Langmuir Probe (PLP) instrument to investigate the horizontal spectrum of density irregularities during large ESF depletions. Our study is complemented by simultaneous high rate (512 Hz) measurements of electric fields made by the VEFI booms.

2.1. Measurements

[6] We focus on measurements made during a strong ESF event observed on the night of October 9–10, 2008 over the

[1]Atmospheric and Space Technology Research Associates, San Antonio, Texas, USA.
[2]School of Electrical and Computer Engineering, Cornell University, Ithaca, New York, USA.
[3]Space Vehicles Directorate, Air Force Research Laboratory, Hanscom Air Force Base, Massachusetts, USA.
[4]NASA Goddard Space Flight Center, Greenbelt, Maryland, USA.

Copyright 2009 by the American Geophysical Union.
0094-8276/09/2009GL038905$05.00

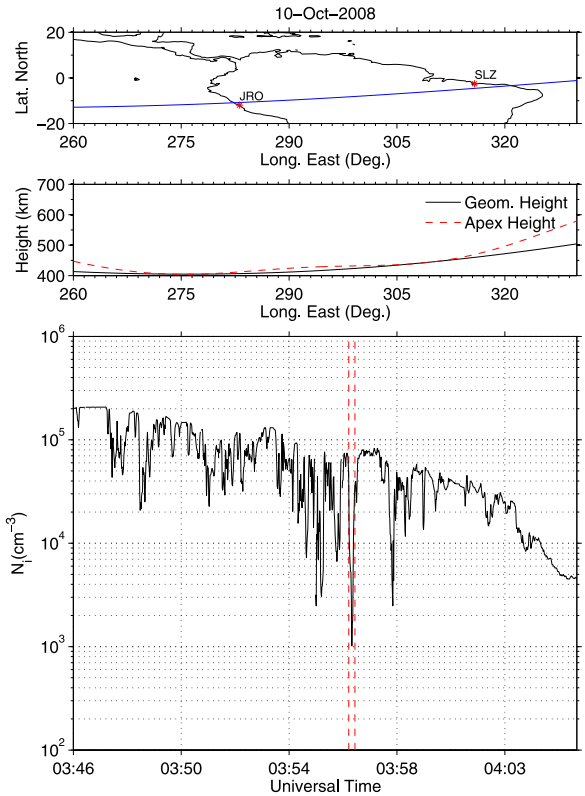

Figure 1. C/NOFS satellite pass over South America on Oct. 10, 2008. (top) Satellite track as a function of latitude and longitude. The location of two equatorial ionospheric radars (Jicamarca - JRO and São Luís - SLZ) are also shown for reference. (middle) Altitude and apex height of the satellite. (bottom) Ion density measurements (1 second averages) made by the PLP instrument indicating the presence of large ESF depletions over South America. The vertical dashed lines indicate the period studied here.

South American longitude sector. These measurements are part of an experimental campaign whose results will be described elsewhere. Figure 1 shows a C/NOFS pass over South America on the night of Oct. 9–10, 2008. The bottom panel shows large ESF density depletions observed by the PLP on that night, especially between 290° and 305° longitude East. The middle panel shows that C/NOFS was flying near its perigee when the density depletions were encountered. Data collected between 03:57:01 UT and 03:57:14 UT (around local midnight) was analyzed and shown in this letter because the satellite was flying through a large ESF depletion (indicated by the vertical dashed lines in the bottom panel of Figure 1, in a trajectory nearly perpendicular to the magnetic field, and because both electric field and density measurements were available for this study.

[7] Figure 2 (top) shows an expanded view of the 512 Hz ion density measurements made by the PLP instrument for the selected time period. Similarly, the zonal component of the electric field measured by VEFI is shown in the bottom panel. This component was obtained from measurements made by two orthogonal double probes in the orbit plane. Figure 2 shows large ion density depletions ($\delta N/N > 98\%$) accompanied by vertical $\mathbf{E} \times \mathbf{B}$ plasma drifts exceeding 200 m/s ($|\mathbf{B}|$ is approximately 22,000 nT).

2.2. Analysis

[8] The procedure used for analysis of both PLP and VEFI data presented in this letter is similar to that used by *Kil and Heelis* [1998] for spectral analysis of the AE-E ion density data. Two seconds (or 1024 data points) of ion density measurements made by the PLP were spectrally analyzed using the Fast Fourier Transform (FFT) algorithm. The FFT is applied to the normalized density deviation ($\delta N/N$), which is computed using a quadratic fit to the data. A Hanning window is applied to the data set before calculating the FFT to avoid spectral artifacts [e.g., *Press et al.*, 1992]. We understand more advanced and accurate methods for spectral analysis exist [e.g., *Chen et al.*, 2001], but for this study, we opted to use the FFT for purposes of comparison with results of previous studies.

3. Results

[9] To illustrate the consistency of our results, Figure 3 (left) show examples of power spectra calculated from the density measurements made by the PLP instrument at six different times during the data interval shown in Figure 2. The spectral densities are plotted as a function of the wavenumber $k = 2\pi/\lambda_{horiz}$. As usual in this type of analysis, k was calculated from the relationship $k = \omega/v$, where ω is the angular frequency of the density fluctuations and v = 7.55 km/s, the mean satellite velocity. We understand that λ_{horiz} is in fact the scale length of the fluctuations in the observables along the satellite orbit. Because the satellite is flying nearly perpendicular to the magnetic field for the case presented here, we assume that $\mathbf{k} \cdot \mathbf{v} \sim |\mathbf{k}||\mathbf{v}|$, and that λ_{horiz} is an estimate of the horizontal (and perpendicular to the magnetic field) wavelength. The title of each panel indicates the starting time of the time series. As mentioned in the Analysis section, the time series used in the FFT computation are 2 seconds (or 1024 points) long.

[10] We are interested in the shape of the density power spectra, and the examples shown in Figure 3 indicate that regions in the spectra tend to follow power laws ($P(k) \propto k^p$, where p is the spectral slope). These examples also show the occurrence of spectral break around k = 90 rad/km (or λ_{horiz} = 70 m). Note that some of the spectra also show

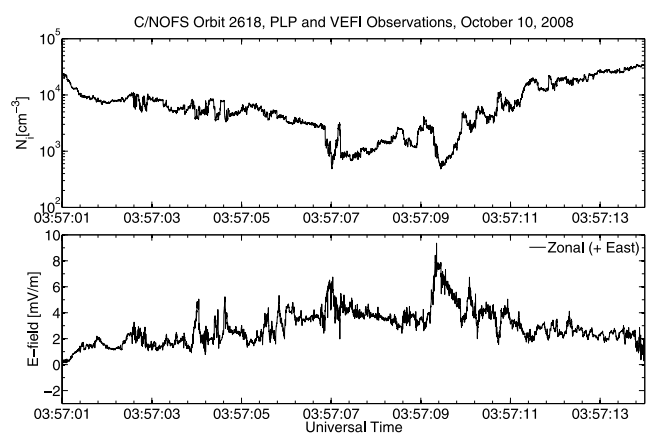

Figure 2. Simultaneous high sampling rate measurements of ion density made by the PLP instrument and zonal electric measurements made by the VEFI instrument between 03:57:01 and 03:57:14 UT.

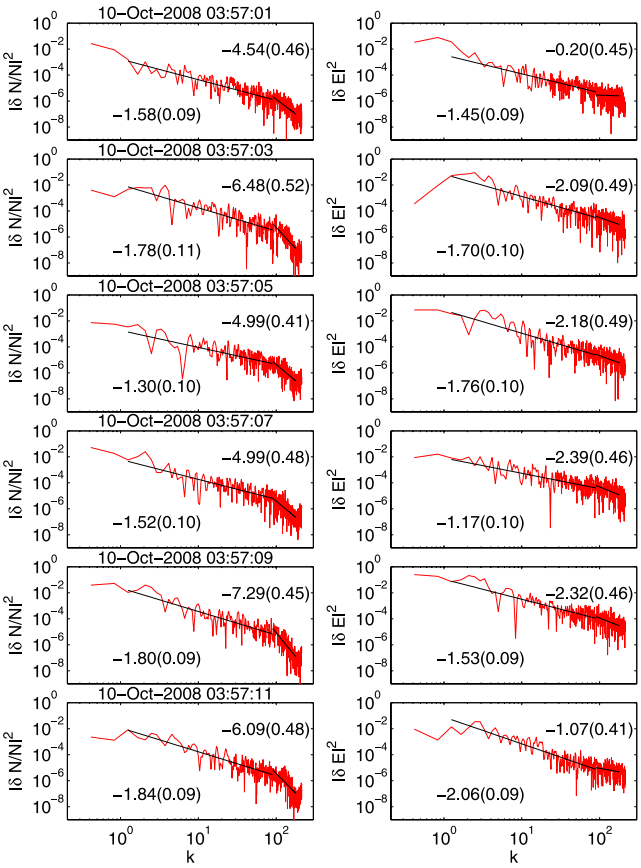

Figure 3. (left) Examples of density power spectra and (right) zonal electric field power spectra. The units for $|\delta N/N|^2$, $|\delta E|^2$, and k are km/rad, $(mV/m)^2$ (km/rad), and rad/km, respectively. The spectral slopes for intermediate and transitional scale-size ranges are shown. The number inside parenthesis is the uncertainty in the estimated spectral slope.

increased spectral densities at the highest frequencies ($k >$ 180 rad/km). This is not a manifestation of any geophysical process. Careful analysis indicated that this is caused by an overcompensation of the instrument spectral response at higher frequencies. This portion of the spectrum is not analyzed and/or discussed in this letter.

[11] Each panel also shows the results of a least squares linear fit. Since the spectrum shows a break around $k =$ 90 rad/km, fits for two separate regions of the spectrum were obtained, one for $1 < k < 90$ rad/km (intermediate scale-sizes) and another one for $90 < k < 180$ rad/km (transitional scale-sizes). The value of the spectral slopes (p) estimated in the fits are indicated in each panel, together with the uncertainty of the estimates (values inside parenthesis).

[12] Figure 3 (right) shows results of the spectral analysis for the fluctuations in the measured zonal electric field. The electric field power spectra was obtained with the same approach used for the density measurements except that the electric field values were not normalized. Spectral slopes and uncertainties are also shown.

4. Discussion

[13] Similarly to what was observed by other satellite missions, regions in the density power spectrum measured by C/NOFS follow a power law. A spectral break at scale-sizes around 70 meters is observed. At intermediate scale-sizes the spectrum is relatively shallow with a spectral slope varying around −5/3. Power density spectra with −5/3 spectral slopes are expected in inertial plasma flows [e.g., *McDaniel and Hysell*, 1997]. This regime, however, is thought to be limited to higher altitudes (>600 km), and earlier local times during normal solar flux conditions [e.g., *Zargham and Seyler*, 1989; *McDaniel and Hysell*, 1997]. We hypothesize that our results might be a manifestation of a secular cooling trend combined with the current solar minimum conditions, which has been leading to the lowest neutral densities in the thermosphere [e.g., *Marcos et al.*, 2008] since the beginning of the space age, and of the unusual late development of ESF.

[14] At transitional scale-sizes, the density power spectrum is very steep with spectral slopes larger than 4. The spectral break is not so obvious in the electric field power spectra. Spectral analysis of rocket observations of ESF irregularities also indicate a spectral break around 80–100 meters [e.g., *Hysell et al.*, 1994]. Our results also confirm the high-sampling rate observations made by the ROCSAT-1 satellite, which indicated an spectral break around 100 meters [*Su et al.*, 2001]. Simultaneous electric field measurements allow us to identify different plasma processes operating in plasma instabilities. Keeping in mind the uncertainties involved in the spectral estimation and spectral slope determination, we found that the slopes in the electric field power spectra tend to follow what was found for the density power spectra in the intermediate scale-size domain. These observations suggest that, at least for intermediate scale-size irregularities, the zonal electric field fluctuations are approximately proportional to the density fluctuations ($|\delta E_{zonal}|^2 \propto |\frac{\delta N}{N}|^2$). This is in agrement with what one would expect for irregularities evolving under the influence of the Rayleigh-Taylor (RT) instability, where one can write $\delta E_{zonal} = -(\frac{gB_o}{\nu_{in}})(\frac{\delta N}{N})$, where $\nu_{\rm in}$ is the ion-neutral collision frequency, B_o is the geomagnetic field intensity, and g is the acceleration due to gravity [e.g., *Kelley*, 1989]. Looking at Figure 2, for instance, we see a strong correlation between kilometric structures in the density and electric field measurements.

[15] At some short wavelength, however, diffusive losses start to overcome the RT instability growth. In this diffusive subrange the density waveform will be similar to the electric potential rather than the electric field. This means that the ratio of the electric field power spectrum to the density power spectrum will not be constant but proportional to k^2. This might explain, at least in part, the differences between the spectral slopes estimated for the density and electric field power spectra in the transitional domain.

5. Conclusions

[16] We presented first results of an analysis of simultaneous, high sampling rate measurements of ion densities and electric fields made by C/NOFS through a large ESF depletion. Spectral analysis have indicated a spectral break in the density power spectrum around 70 m. These observations are in agreement with previous observations made by rockets and satellites [e.g., *Hysell et al.*, 1994; *Su et al.*, 2001]. We suggest that the spectral break is a result of a

diffusive subrange. We also found that the spectral slopes at intermediate scale-sizes is approximately $-5/3$. Density spectra with $-5/3$ spectral slopes are believed to be found in observations of large ESF plasma depletions in the topside ionosphere at high altitudes. Our results, however, were found for measurements made at relatively low altitudes ($\sim$450 km). We hypothesize that this could be a result of the long-lasting solar minimum conditions leading to much lower neutral densities (and ν_{in} values) than usually seen. This would bring the transition from the collisional to inertial regime to a much lower altitude. More definitive results about the occurrence of inertial plasma flows as a result of the current solar flux conditions, however, will require and motivated us to carry out further analyses with a larger number of C/NOFS observations aided by numerical models such as those developed by *McDaniel and Hysell* [1997] and *Hysell and Shume* [2002].

[17] The results presented in this letter are relevant for a better modeling of radio wave scintillation, one of the main goals of the C/NOFS mission. The intensity of VHF/UHF scintillations observed by ground-based receivers depends on the magnitude and spectral distribution of density fluctuations in the intermediate and transitional domains.

[18] **Acknowledgments.** The C/NOFS mission is supported by the Air Force Research Laboratory, the Department of Defense Space Test Program, the National Aeronautics and Space Administration (NASA), the Naval Research Laboratory, and the Aerospace Corporation. Research at ASTRA was partly funded by NSF Award ATM-0719872. Research at Cornell University was supported by the Air Force Office of Scientific Research Award FA9550-05-0160.

References

Chen, K. Y., H. C. Yeh, S. Y. Su, C. H. Liu, and N. E. Huang (2001), Anatomy of plasma structures in an equatorial spread F event, *Geophys. Res. Lett.*, *28*(16), 3107.

de La Beaujardière, O., et al. (2004), C/NOFS: A mission to forecast scintillations, *J. Atmos. Sol. Terr. Phys.*, *66*(17), 1573.

Hysell, D. L., and E. B. Shume (2002), Electrostatic plasma turbulence in the topside equatorial F region ionosphere, *J. Geophys. Res.*, *107*(A10), 1269, doi:10.1029/2001JA000227.

Hysell, D. L., M. C. Kelley, W. E. Swartz, R. F. Pfaff, and C. M. Swenson (1994), Steepened structures in equatorial spread F: 1. New observations, *J. Geophys. Res.*, *99*(A5), 8827.

Kelley, M. C. (1989), *The Earth's Ionosphere: Plasma Physics and Electrodynamics*, Academic, San Diego, Calif.

Kil, H., and R. A. Heelis (1998), Equatorial density irregularity structures at intermediate scales and their temporal evolution, *J. Geophys. Res.*, *103*(A3), 3969.

Marcos, F. A., B. R. Bowman, N. J. Grossbard, and S. H. Delay (2008), Thermospheric neutral density cooling trends: 1962–2008, *Eos Trans. AGU*, *89*(53), Fall Meet. Suppl., Abstract SA21B-1562.

McDaniel, R. D., and D. L. Hysell (1997), Models and DE II observations of inertial-regime irregularities in equatorial spread F, *J. Geophys. Res.*, *102*(A10), 22,233.

Press, W., S. A. Teukolsky, W. T. Vetterling, and B. P. Flannery (1992), *Numerical Recipes*, 2nd ed., Cambridge Univ. Press, Cambridge, U. K.

Su, S.-Y., H. C. Yeh, and R. A. Heelis (2001), ROCSAT 1 ionospheric plasma and electrodynamics instrument observations of equatorial spread F: An early transitional scale result, *J. Geophys. Res.*, *106*(A12), 29,153.

Zargham, S., and C. E. Seyler (1989), Collisional and inertial dynamics of the ionospheric interchange instability, *J. Geophys. Res.*, *94*(A7), 9009.

G. S. Bust and F. S. Rodrigues, ASTRA, 12703 Spectrum Drive, Suite 101, San Antonio, TX 78249, USA. (frodrigues@astraspace.net)

O. de La Beaujardière, D. E. Hunton, and P. A. Roddy, Space Vehicles Directorate, Air Force Research Laboratory, 29 Randolph Road, Hanscom Air Force Base, MA 01731, USA.

M. C. Kelley, School of Electrical and Computer Engineering, Cornell University, 318 Rhodes Hall, Ithaca, NY 14853, USA.

R. F. Pfaff, NASA Goddard Space Flight Center, Mail Code 674, Greenbelt, MD 20771, USA.